Acta Geologica Sinica (English Edition), 2019, 93(4): 1149–1151

Research Advances

New Zircon U-Pb Ages of Mylonitic Granite in the Baluntai Area of the Central Tianshan Block and their Geological Implications

TAO Zaili[1, 2], YIN Jiyuan[2, *], CHEN Wen[2], LI Dapeng[1], CAI Keda[1], XU Zhihua[1, 2] and DU Qiuyi[2]

[1] *School of Earth Sciences and Resources, China University of Geosciences, Beijing, 100083, China*
[2] *Key Laboratory of Deep-Earth Dynamics of Ministry of Natural Resources, Institute of Geology, Chinese Academy of Geological Sciences, Beijing 100037, China*

Citation: Tao et al., 2019. New Zircon U-Pb Ages of Mylonitic Granite in the Baluntai Area of the Central Tianshan Block and their Geological Implications. Acta Geologica Sinica (English Edition), 93(4): 1149–1151. DOI: 10.1111/1755-6724.14313

Objective

The central Tianshan block mainly consists of the Precambrian metamorphic basement, Ordovician–Silurian meta-sedimentary rocks and Carboniferous–Permian sedimentary rocks. The Precambrian metamorphic basement is predominately composed of amphibolite- and granulite-facies metamorphic rocks, including sillimanite-biotite-quartz schists, garnet-plagioclase granulites, granitic gneisses, amphibolites, migmatites and marbles. The Paleozoic granitoids are widely distributed in the central Tianshan block and intruded into the Precambrian metamorphic basement and earlier sedimentary rocks. However, some Paleozoic granitoids have experienced a high deformation and metamorphism in later tectonic events, and they are therefore difficult to be distinguished with Precambrian granitoids. As a result, many deformed Paleozoic granitoids were classified as a part of the Precambrian metamorphic basement on the K-45-IX geological maps (1:200, 000) of the central Tianshan block. Obviously, high-precision zircon U-Pb dating is necessary to determine the crystallization age of the various deformed granitoids. In this study, we present new zircon U-Pb ages for the Baluntai mylonitic granite exposed in the central Tianshan block in order to test their possible formation ages and to further understand the Paleozoic magmatism and tectonic evolution of the central Tianshan block.

Methods

The sample CT1614 (Fig. 1a–b) of the mylonitic granite (N42° 45′23″, E86° 18′24″) was collected in the southwest part of the Baluntai Town. It belongs to the Precambrian metamorphic basement in the K-45-IX geological maps (1: 200, 000). The contact relationship between the mylonitic granite and the metamorphic basement was not directly observed. The mylonitic granite is grey and consists mainly of plagioclase (40 vol.%), alkali feldspar (30 vol.%), quartz (20 vol.%), and biotite (5 vol.%); the K-feldspar and plagioclase minerals display augen structures indicative of its magmatic origin. The LA-ICP-MS U-Pb dating for the sample CT1614 was conducted using an Agilent 7500a ICP-MS with an attached 193 nm excimer ArF laser-ablation system (GeoLas Plus) at the Institute of Geology and Geophysics, Chinese Academy of Sciences. LA-ICP-MS zircon U-Pb isotopic data are presented in Appendix 1.

Results

Twenty-five zircon grains from the mylonitic granite (sample CT1614) were used for U-Pb dating. Zircon grains are colorless, transparent to translucent with lengths ranging from 150 to 300 μm and widths from 100 to 200 μm, and length/width ratios of 2:1 to 3:1 (Fig. 1a). The CL images show mostly euhedral and obvious oscillatory zoning, with high Th/U ratios (0.17–0.98) (Appendix 1). In addition, their REE patterns are typically characterized by enrichment in HREE with positive Ce anomalies and negative Eu anomalies (Appendix 1; Fig.1b), similar to those of magmatic zircons (Appendix 2). The results of the 25 U-Pb ages in the sample CT1614 are relatively concordant and have a weighted mean $^{206}Pb/^{238}U$ age of 429.8±1.9 Ma (MSWD=0.22) (Fig. 1a). We interpret this as the crystallization age of the mylonitic granite, suggesting that it was formed in the Early Silurian, but not in the Precambrian as previously (K-45-IX) (1:200,000) assumed. Many amphibolites- and granulite-facies metamorphic rocks are exposed in the ductile shear zone in the Baluntai area. The metamorphic rocks were previously accepted to be part of the Precambrian metamorphic basement since they show various degrees of gneissic foliation, lineation and directional structures. These characteristics suggest that they have experienced various degrees of ductile deformation. However, the Paleozoic rocks have also witnessed important deformation and metamorphism. Thus, they are not easily distinguished with the Precambrian metamorphic basement, especially on the outcrops. It is exemplified by petrological observations without geochronological study.

* Corresponding author. E-mail: yinjiyuan1983@163.com

http://www.geojournals.cn/dzxbcn/ch/index.aspx; https://onlinelibrary.wiley.com/journal/17556724

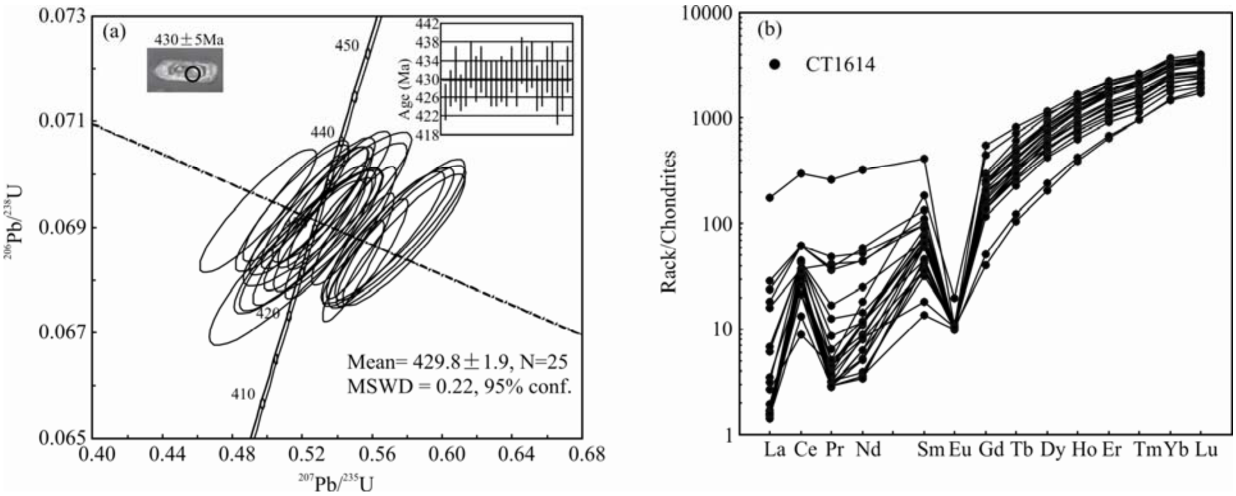

Fig. 1. (a) Zircon U-Pb concordia plot for the mylonitic granite; (b) chondrite-normalized REE patterns of zircons (Data from Appendix 2).

Obviously, more zircon U-Pb dating is required to confirm the formation age of the metamorphic rocks in the central Tianshan block. In addition, the Silurian (430.1±1.1 Ma) diorite exposed along the Baluntai area are calc-alkalic and have obvious enrichments in LREE and LILE, and depletions in HSFE, showing typical characteristics of arc magmatism affinity. Therefore, the Paleozoic metamorphic rocks could be closely related to the subduction of the Pale-oasian ocean slab.

Conclusions

(1) LA-ICP-MS zircon dating suggests that the deformed granitic plutons were emplaced in the Early Silurian (429.8±1.9 Ma), instead of the Precambrian.

(2) The mylonitic plutons have experienced various degrees of ductile deformation and metamorphism related to the subduction of the ocean slab.

Acknowledgements

This study was financially supported by the China Geological Survey (grants No. DD20190001, DD20190004), the Fund from the Key Laboratory of Deep -Earth Dynamics of Ministry of Natural Resources and the National Science Foundation of China (grants No. 41473053, 41573045, 41873060 and 41830216). This is a contribution to the IGCP-Project 662.

Appendix 1 Zircon isotopic analyses for the mylonitic granite in the Baluntai area of the central Tianshan block

Analysis spots	Content (ppm)			Isotopic ratios						Intercept age (Ma)			
	Th	U	Th/U	$^{207}Pb/^{235}U$	1σ	$^{206}Pb/^{238}U$	1σ	$^{207}Pb/^{206}Pb$	1σ	$^{207}Pb/^{235}U$	1σ	$^{206}Pb/^{238}U$	1σ
WT1614-01	837	1861	0.45	0.54914	0.01165	0.06818	0.00064	0.05848	0.00118	444	8	425	4
WT1614-02	592	1388	0.43	0.55311	0.01277	0.06864	0.00066	0.0585	0.0013	447	8	428	4
WT1614-03	218	567	0.38	0.54158	0.02534	0.06918	0.00093	0.05683	0.00267	439	17	431	6
WT1614-04	537	1503	0.36	0.55978	0.01349	0.06852	0.00067	0.0593	0.00137	451	9	427	4
WT1614-05	166	958	0.17	0.53483	0.01643	0.06879	0.00076	0.05642	0.00171	435	11	429	5
WT1614-06	135	669	0.20	0.52908	0.02145	0.06945	0.00082	0.05528	0.00223	431	14	433	5
WT1614-07	320	594	0.54	0.57545	0.02451	0.06895	0.00088	0.06056	0.00258	462	16	430	5
WT1614-08	495	1049	0.47	0.53589	0.01606	0.06936	0.00077	0.05605	0.00164	436	11	432	5
WT1614-09	449	1133	0.40	0.5495	0.01593	0.06902	0.00074	0.05775	0.00162	445	10	430	4
WT1614-10	294	629	0.47	0.56657	0.023	0.06878	0.00084	0.05973	0.00239	456	15	429	5
WT1614-11	309	647	0.48	0.57789	0.02301	0.06876	0.00082	0.06094	0.00238	463	15	429	5
WT1614-12	295	801	0.37	0.52769	0.01944	0.06898	0.00078	0.05546	0.00198	430	13	430	5
WT1614-13	257	562	0.46	0.57412	0.02593	0.06882	0.00089	0.06048	0.00269	461	17	429	5
WT1614-14	427	1055	0.40	0.53169	0.01699	0.06938	0.00076	0.05555	0.00167	433	11	432	5
WT1614-15	260	546	0.48	0.5229	0.02573	0.06875	0.00088	0.05513	0.00266	427	17	429	5
WT1614-16	344	708	0.49	0.53646	0.02227	0.06957	0.00082	0.05589	0.00224	436	15	434	5
WT1614-17	310	813	0.38	0.51447	0.02149	0.06936	0.00079	0.05376	0.00216	421	14	432	5
WT1614-18	399	966	0.41	0.51613	0.01991	0.0695	0.00076	0.05382	0.00194	423	13	433	5
WT1614-19	439	845	0.52	0.52376	0.02122	0.0687	0.00078	0.05525	0.0021	428	14	428	5
WT1614-20	788	801	0.98	0.56878	0.02509	0.06884	0.00085	0.05988	0.00251	457	16	429	5
WT1614-21	321	855	0.38	0.52356	0.02248	0.06931	0.0008	0.05475	0.00221	428	15	432	5
WT1614-22	447	457	0.98	0.53427	0.03181	0.06934	0.00096	0.05584	0.00324	435	21	432	6
WT1614-23	225	544	0.41	0.51639	0.03285	0.06844	0.00111	0.05468	0.00342	423	22	427	7
WT1614-24	211	629	0.34	0.52318	0.02813	0.06873	0.0009	0.05517	0.00284	427	19	428	5
WT1614-25	334	873	0.38	0.49474	0.02194	0.0693	0.00077	0.05174	0.00212	408	15	432	5

Appendix 2 REE compositions (ppm) of zircons from the mylonitic granite in the Baluntai area of the central Tianshan block

Analysis spots	La	Ce	Pr	Nd	Sm	Eu	Gd	Tb	Dy	Ho	Er	Tm	Yb	Lu
WT1614-01	3.83	22.95	4	20.61	17.48	<0.59	63	23.11	268	91.17	369.2	68.91	611.5	98.14
WT1614-02	5.68	38.22	4.68	24.93	15.26	<0.62	50.67	17.79	207.3	72.16	299.9	59.9	562.1	95.15
WT1614-03	0.83	17.49	0.35	3.77	5.69	<0.62	28.49	9.92	113.6	40.06	167.9	34.13	330.3	57.02
WT1614-04	41.88	186.78	25.48	153.8	63.34	<0.62	114.3	31.4	301.2	96.29	376.1	68.69	597.8	93.8
WT1614-05	0.63	5.51	0.42	3.86	2.78	<0.60	8.44	4.02	52.85	22.08	108.1	25.16	264.1	48.29
WT1614-06	<0.35	8.16	<0.28	<1.70	<2.12	<0.58	10.75	4.72	61.36	24.53	116	24.99	257.2	45.29
WT1614-07	0.46	16.24	0.48	4.21	9.27	<0.65	49.56	16.1	195.1	69.28	287.3	56.53	538.6	92.29
WT1614-08	1.46	26.81	1.63	11.67	10.66	<0.63	39.57	13.81	167.7	57.88	240.1	47.06	461.3	73.24
WT1614-09	<0.40	19.72	<0.31	<1.84	4.98	<0.65	36.06	13.76	180.7	65.59	277.8	52.66	506.3	82.31
WT1614-10	<0.35	17.68	0.41	5.13	12.07	<0.58	58.37	19.91	238.2	83.18	342	64.35	601.9	99.54
WT1614-11	<0.37	20.42	0.36	5.39	10.7	0.64	48.78	15.61	189.4	67.08	277	52.38	498.3	84.14
WT1614-12	6.79	38.8	3.51	21.1	15.27	<0.58	40.84	12.97	150.3	51.57	212.9	41.26	410.8	66.61
WT1614-13	<0.36	13.12	<0.28	<1.68	5.87	<0.57	29.82	10.51	128.4	45.63	193.6	37.6	372.8	63.92
WT1614-14	<0.37	18.38	<0.30	3.93	10.56	<0.61	48.38	18.15	233.7	85.32	355.1	67.29	646.8	105.1
WT1614-15	<0.36	13.32	0.43	5.5	14.1	<0.59	53.54	18.64	223.5	76.88	317.8	58.27	574.7	93.74
WT1614-16	<0.37	23.16	0.62	5.63	11.56	<0.60	53.69	18.33	216.1	75.1	307.1	57.36	560.6	89.02
WT1614-17	<0.39	18.34	<0.30	2.46	9.38	<0.63	43.48	15.15	192.9	67.82	290.4	54.52	538.4	87.68
WT1614-18	<0.37	21.73	<0.28	2.39	6.52	<0.58	31.04	12.14	157.4	54.92	232.6	43.7	447.9	71.47
WT1614-19	<0.39	27.46	0.48	8.51	28.7	1.14	93.76	27.07	284.7	83.99	319.2	56.68	553	87.14
WT1614-20	1.62	26.15	1.19	6.68	9.26	<0.59	35	12.43	156.2	51.19	212.8	40.23	412.6	65.59
WT1614-21	<0.36	21.88	<0.28	2.95	5.45	<0.60	30.91	11.36	148.6	51.51	224.5	42.02	441.8	71.48
WT1614-22	0.75	27.74	0.82	5.49	7.04	<0.57	24.49	8.77	109.1	35.78	154.9	29.46	310.7	50.73
WT1614-23	<0.34	16.19	<0.267	2.91	10.03	<0.57	28.8	10.15	133.5	45.67	192.1	36	376.9	61.08
WT1614-24	4.37	38.78	3.73	27.75	21.03	<0.59	42.42	12.2	134.2	43.07	175.6	33.1	346.5	55.67
WT1614-25	<0.37	22.03	<0.28	<1.61	7.13	<0.61	29	11.25	149.9	51.59	222	41.67	437	70.26